Establishment and characterization of oxaliplatin-resistant human colorectal cancer cell line

Amanda A. C. Morais[1], Karina Neres[1], Ygor F. Nogueira[1], Renato K. A. de O. França[2], Rayane Ganassin[1], Patrícia B. da Silva[1], Andrea Q. Maranhão[2], Ricardo B. de Azevedo[1*].

1Nanoscience and Nanobiotechnology Laboratory, Department of Genetics and Morphology, Institute of Biological Sciences, University of Brasilia, Brasilia/DF, Brazil.
2Molecular Biology Laboratory, Department of Cell Biology, Institute of Biological Sciences, University of Brasilia, Brasilia/DF, Brazil.

Abstract:
Background: The acquisition of chemoresistance is one of the most concerning challenges in anti-cancer therapy. Despite being used as the first-line treatment for advanced or metastatic colorectal cancer, the development of resistance to oxaliplatin (L-OHP) is a problem that affects many patients treated with this drug.This study aimed to describe and characterize the establishment of an oxaliplatin (L-OHP) resistant colorectal cancer cell line (HCT116-R).
Materials and Methods: The HCT116-R cell line was obtained through prolonged exposure to gradually increasing L-OHP concentrations. The growth activity, tumor spheroid formation capacity, cell cycle, and cell death were analyzed.
Results: After acquiring resistance, cells showed a significant change in their doubling time and growth rate when exposed to different L-OHP concentrations. HCT116-R cells are more efficient in forming tumor spheres, even after exposure to high L-OHP concentrations, when compared to a sensitive cell line (HCT116-S). HCT116-R cells seemed to evade apoptosis and cell cycle arrest with an increased percentage of cells in the G0/G1 phase, even when exposed to high L-OHP concentrations, and an increased proportion of cells in the G2/M phase after exposure to the highest L-OHP concentration. HCT116-S cells presented increased apoptosis in addition to a high incidence in the sub-G1 phase when exposed to any L-OHP concentration.
Conclusion:The prolonged exposure with a gradual increase in L-OHP concentration used herein is feasible to reproduce, and the characteristics observed for the resistant cell line are consistent with the profile expected for resistant cells. This model can be used to better understand the biological response behind resistance, how new treatments could improve the response to chemotherapy with L-OHP, and contribute to discovering possible therapeutic biomarkers for a resistance model.
Key Word:CRC, drug resistance, colorectal cancer resistance, L-OHP, platinum compounds.

Date of Submission: 14-04-2023   Date of Acceptance: 27-04-2023

I. INTRODUCTION

Colorectal cancer (CRC) is a multifactorial disease of the digestive tract affecting both the colon and rectum that can be influenced by genetic factors (heredity) and factors relating to lifestyle, diet, and obesity[1-4]. Standard CRC treatment consists of surgery involving the mechanical removal of polyps/tumors, and is often associated with systemic chemotherapy and/or radiotherapy regimens before or after their removal[1,5-7]. Depending on the cancer stage, other therapies may be combined to improve treatment, for example in cases involving patients with advanced or metastatic CRC in which immunotherapy targeting the tumor molecular profile may be employed[7,8,9].Despite advances, drug resistance remains a common challenging occurrence in CRC patients, resulting in loss of treatment efficacy and, consequently, recurrence in a more aggressive and lethal profile[6,8,10-12] with a median 5-year survival rate for only 10% of patients[2,13,14].

One of the most used chemotherapy drugs in metastatic CRC is oxaliplatin (L-OHP), a third-generation platinum agent. L-OHP is a therapeutic improvement over first- and second-generation platinum agents, such as cisplatin and carboplatin, respectively[15,16]. L-OHP is an alkylating agent with an oxalate group and a DACH carrier ligand (diaminocyclohexane) enabling the formation of covalent bonds with DNA (DNA adducts), leading to a cascade of failures in important cellular processes and, consequently, cell death by apoptosis and necrosis[17-20]. The introduction of L-OHP as a first or second-line therapy for advanced or metastatic tumors has significantly increased patient survival rate. It is noteworthy that it can be improved when used in combination

---

chemotherapy regimens, such as when associated with the drugs 5-fluorouracil and leucovorin. However, there is still a 40% resistance rate in patients[18,19].

As most treatments are performed in long-term regimens, the remaining cells change over time, absorb the chemotherapy in a smaller amount, and acquire other mutations favorable to the resistance profile[21]. The new profile can be caused by intrinsic or acquired factors and mediated by factors external/internal to the cell or in its membrane [22,23].The acquisition of drug resistance profiles by cancer cells is known as multidrug-resistance (MDR) which is characterized by the development of several mechanisms enabling cancer cells to circumvent the effects of anti-cancer drugs, thereby resulting in treatment failure and increased malignancy[23,24]. Noteworthy characteristics involved in the MDR profile include: (1) altered apoptotic pathways, such as the increase of the proteins involved in DNA repair; (2) increased drug metabolism or inactivation; (3) over-expression of efflux pumps on the cell membrane, associated with decreased drug influx, and (4) alteration of cell cycle checkpoints; among others[23,25-29].

Establishing an in vitro model of L-OHP resistant CRC is an important contribution to the knowledge about the biology and treatment of MDR CRC. Thus, the present study aimed to describe the development and characterization of a resistant CRC cell line model by prolonged exposure to gradually increasing L-OHP concentrations, fostering future studies into new treatments and the molecular profile behind the therapeutic response.

II. MATERIAL AND METHODS

Cell culture

The human colorectal carcinoma cell line (HCT116) was kindly provided by Dr. Leticia Veras Costa Lotufo (Institute of Biomedical Sciences, University of São Paulo, SP). Cells were cultured in RPMI-1640 medium (Sigma Aldrich) supplemented with 10% fetal bovine serum and 1% (v/v) penicillin/streptomycin (GIBCO), in a controlled incubator (37 °C, humidified atmosphere with 5% CO2), and subcultured on reaching 80% confluence.

Determination of oxaliplatin half-maximal inhibitory concentration (IC50)

To determine the L-OHP half-maximal inhibitory concentration (IC50), HCT116 cells were plated in a 96-well plate at a density of 1×10^4 cells/well 24 h before exposure to increasing (2, 5, 10, 20, 30, 40, 60, 80, 100, and 120 µM) L-OHP concentrations (Energy Chemical, China. Cat. No. E0215670050, CAS No. 61825-94-3) diluted in the medium. After 48 h of exposure, cytotoxicity was analyzed using the MTT tetrazolium salt colorimetric assay (5 mg/mL, Invitrogen, USA)[30]. The IC50 value was obtained by comparing the dose-survival curve to the group of cells exposed to culture medium only (control).

Resistant cell line establishment

The induction of the L-OHP-resistant cell line (HCT116-R) followed the protocol of prolonged exposure with gradual increases in L-OHP concentration[31]. Throughout the HCT116-R cell line establishment, the parental cell line was exposed to the standard culture medium as a control/sensitive group (HCT116-S). After IC50 determination, the cells were cultured in T75 bottles and, after reaching 60% confluence, exposed to an initial L-OHP concentration corresponding to 1/3 of the IC50 diluted in the culture medium. After 48 h of drug exposure, the culture medium was changed to the standard medium without L-OHP. After reaching 80% confluence, cells were subcultured and treated with the same initial L-OHP concentration. This procedure was repeated once more, totaling 3 times for each concentration, after which the concentration was doubled and the procedure repeated for each new concentration.

The HCT116-R cell line was established after the concentration equivalent to 10x the IC50 value and sporadically exposed to a medium containing 4 µM L-OHP to maintain resistance. Cells were cultured until 10 passages after the establishment.

Growth analysis: trypan blue exclusion assay

To identify changes in doubling time, HCT116-S and HCT116-R cell growth times were compared. For this, 2×10^3 cells were cultured in 6-well plates in triplicate and maintained for 120 h, with the medium renewed every 48 h. The viable cell number was determined using trypan blue staining and a Neubauer camera, counting every 24 h until reaching 120 h using a double-blind counting system. Finally, the doubling time was calculated by using an algorithm available online[32].

Real-time growth assay

The growth of each cell line exposed to L-OHP, HCT116-S and HCT116-R, was analyzed in real-time by the xCELLigence RTCA DP system (Roche, San Diego, CA, USA), using 16-well plates containing gold electrodes at the bottom (E-Plate 16). Five experimental groups were used: (1) control: cells exposed to standard

medium; (2) L-OHP 5 µM: cells exposed to L-OHP 5 µM; (3) L-OHP 50 µM: cells exposed to L-OHP 50 µM; (4) L-OHP 100 µM: cells exposed to L-OHP 100 µM, and (5) Blank: medium without cells to control the impedance signal.

Briefly, 50 µL of the medium was added to each well to set the equipment for 10 min. Shortly after, the reading was paused, and 100 µL of medium containing $2x10^3$ cells was added. Thirty minutes after adding the cells to the wells, the plates were placed in the RTCA. The equipment was calibrated for 10 min, followed by cell index (CI) acquisition by measuring the impedance every 30 min for 120 h. The reading was paused after 24 h to change the medium with/without treatment, according to each group. After 48 h of exposure to the treatments, reading was paused, the medium was replaced with standard medium, and reading restarted until completion of 120 h.

Tumor spheroid formation assay

To analyze spheroid formation, 3D assays of the HCT116-S and HCT116-R cell lines were performed in the presence of L-OHP over 7 days, following the methodology previously described[33]. Briefly, cells were plated at a density of 2,000 cells per well in a 96-well plate modified with 50 µL of low melting agarose 1.5 % (wt/vol) (Invitrogen). The plates were stored in the cell incubator to allow sphere formation for 4 days after which time they were photographed using an inverted microscope (Invitrogen™ EVOS™ FL Auto Imaging System) and had the culture medium changed, as follows: (1) control: cells exposed to standard medium; (2) L-OHP 5 µM: cells exposed to 5 µM L-OHP; (3) L-OHP 50 µM: cells exposed to 50 µM L-OHP, and (4) L-OHP 100 µM: cells exposed to 100 µM L-OHP. Finally, after 7 days, cells were rephotographed.

The photos were analyzed using the free ImageJ software to measure the spheroid horizontal diameter of each cell line and calculate the total area (spheroid contour and value in pixels). In addition, spheroidal growth rate was determined using the pixel value on day 4 and day 7 for each group.

Cell cycle analysis: flow cytometry

A concentration of $1x10^5$ cells from each cell line exposed to L-OHP (0 µM, 5 µM, 50 µM, and 100 µM) for 48 h was centrifuged, with the resulting pellet washed with PBS, and recentrifuged. The supernatant was removed. The cells were fixed with 1 mL of ice-cold 70% ethyl alcohol at -20 °C overnight. The cell pellet was washed with PBS and incubated with a solution of ribonuclease A (RNase A, 0.05%) and propidium iodide (50 µg/mL). The cells were analyzed using a flow cytometer (BD Accuri™ C6 Plus Flow Cytometer, USA). Cell cycle analysis was performed using the FlowJo™ Software.

Cell death analysis: flow cytometry

Similar to the previous assay, $1x10^5$ cells from each cell line exposed for 48 h to L-OHP (0 µM, 5 µM, 50 µM, and 100 µM) were centrifuged and washed with PBS. Cell death was assessed using the Annexin V-FITC Apoptosis Detection Kit (Invitrogen™), following the manufacturer's instructions. Briefly, the cells were resuspended in binding buffer, prior to exposure to markers, kept on ice, and incubated for 15 min in the dark in 5 µL annexin-V-FITC. After a short period, the cells were subsequently exposed to 10 µL propidium iodide (20 µg/mL), and analyzed using a flow cytometer (BD Accuri™ C6 Plus Flow Cytometer, USA). The data was analyzed using the FlowJo™ Software.

Statistical analysis

Statistical analysis was performed using the GraphPad Prism 6 software (GraphPad Software, USA). The Student's t-test was used to compare the means between the 2 groups, together with analysis of variance (ANOVA) and the post-hoc Tukey test to compare more than 2 groups, always considering a 95% confidence interval.

III. RESULT

Resistant cell line establishment

Initially, the L-OHP IC_{50} value for the parental cell line (HCT116-S) was 2.8±0.04 µM at passage 1 (P1). Thus, cell line establishment was started with 1 µM and ended after reaching a 30 µM L-OHP in the culture medium. The total exposure time to obtain the HCT116-R cell line was approximately 11 months. It is important to note that in the first exposure to chemotherapy, the cell line was at passage 7 (P7) and after reaching the final resistance value, the HCT116-R cell line was at P40. A control bottle of HCT116-S, exposed to the standard culture medium only was maintained throughout the entire resistance induction period, ending at the same passage number. Both cell lines were used for no more than 10 passages after establishment.

The final resistance result is described in Fig. 1, shows the difference between the IC_{50} of each cell line, which is 2.7±0.3 µM for the HCT116-S cell line and 26.6±1.5 µM for the HCT116-R cell line (Fig. 1a).

Thedrug resistance index is equal to 10.2±1.0, demonstrating that the HCT116-R cell line is significantly resistant to L-OHP (P<0.001) (Fig. 1b).
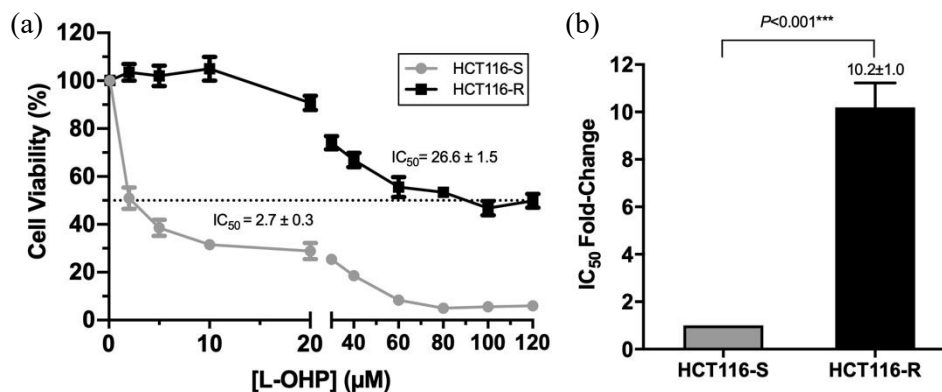
Figure 1. Viability analysis after the establishment of resistant cell line by gradual exposition to L-OHP. (a) Exposition to L-OHP for 48 h to determine the IC_{50}. Dotted line represents the viability of 50% of the cells. (b) Drug resistance index. Results expressed as mean ±SEM (standard error of the mean) of3 independent experiments performed in triplicate. Student's t-test: **P<0.001

Growth analysis using trypan blue exclusion assay and real-time growth assay

The doubling time of the HCT116-R cell line is 26.89±0.8 h, significantly higher (P>0.001) than the time that the HCT116-S cell line takes to double (19.29±0.9 h) (Fig.2a). HCT116-R cells showed slower growth than parental cells (HCT116-S), both in the trypan blue exclusion assay (Fig.2b) and in the real-time growth assay (Fig.3).
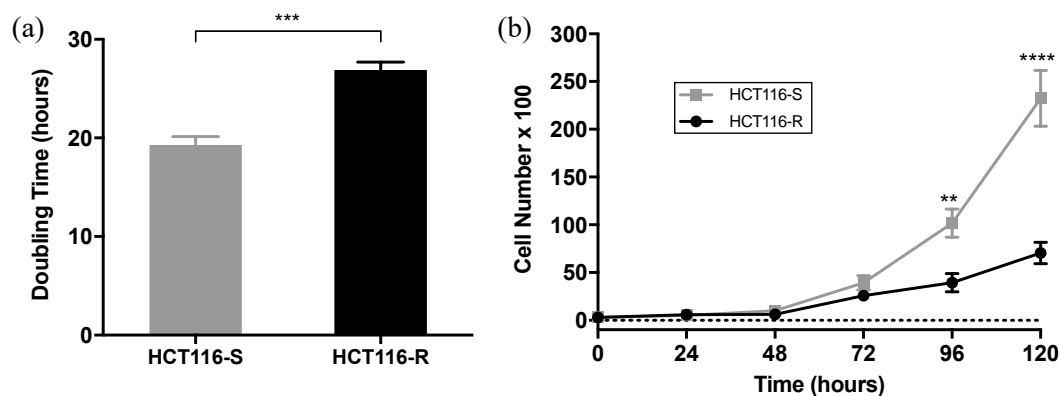
Figure2. Cell growth analysis. (a) Average doubling time for each cell line, using the average time obtained by trypan blue counting and real-time analysis; (b) Cell number determined by trypan blue exclusion assay over 120 h. Results expressed as mean ±SEM of3 independent experiments performed in triplicate. Student's t-test: **P<0.01; ***P<0.001; ****P<0.0001

The HCT116-S cells showed a cell index drop 16 h (death onset time) after exposure to the highest L-OHP concentrations (50 and 100 µM) and a cell index drop 28 h after exposure to 5 µM L-OHP(Fig. 3a), the drop was continuous until the cellular index value was close to zero and similar to the negative control (blank group) (Fig.3a and 3c). In contrast, the HCT116-R cells presented continuous growth in the presence of 5 µM L-OHP, and at the highest concentrations (50 and 100 µM) was observed to enter a latency state (Fig.3b and 3c).
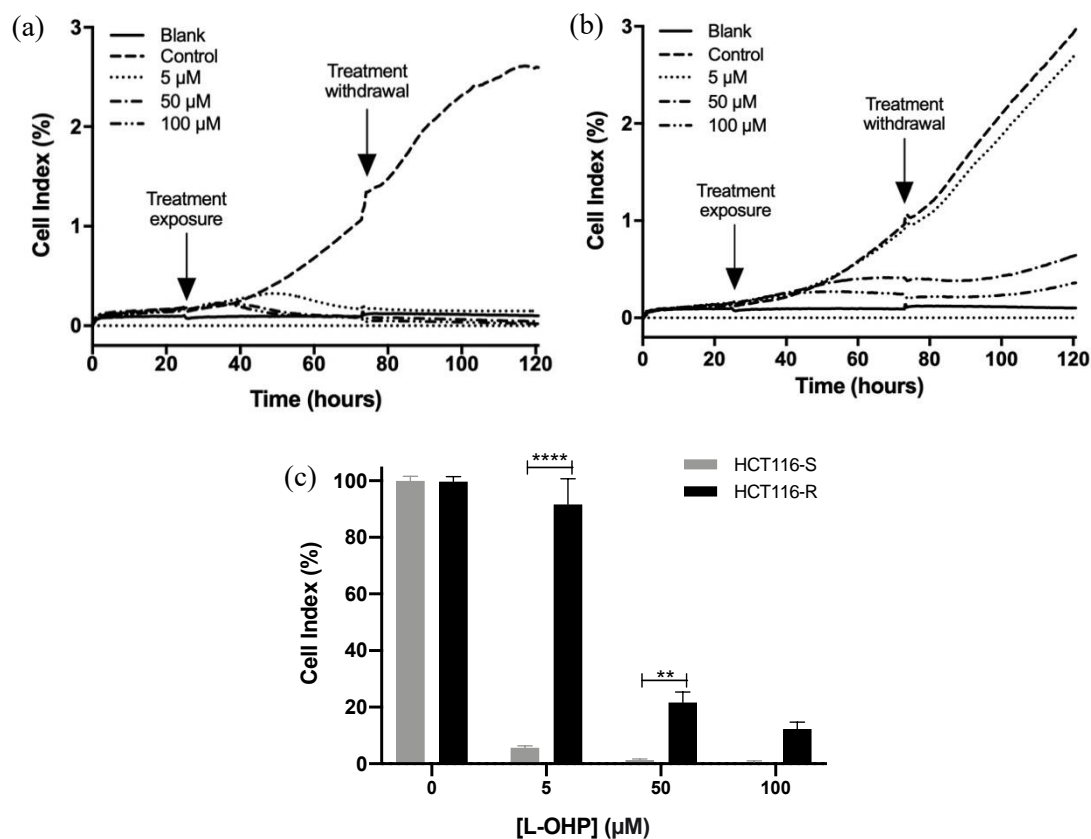
Figure3. Real-time cell growth analysis. (a) HCT116-S real-time growth curve after exposure to different L-OHP concentrations. (b) HCT116-R real-time growth curve after exposure to different L-OHP concentrations; (c) Cell index percentage at the end of 120 h in the presence/absence of L-OHP. Results expressed as mean ±SEM of3 independent experiments performed in triplicate. ANOVA two-way: **$P<0.01$; ****$P<0.0001$

Tumor spheroid formation assay

Fig. 4a shows the spheroid photomicrographs after 4 days of growth (without treatment), followed by the same spheroids 3 days after the addition of each treatment (total of 7 days of growth). After exposure to the higher L-OHP concentrations (50 and 100 µM), spheroids formed by HCT116-S cells demonstrated a statistically significant reduction in their total area (Fig.4b). This reduction can be observed in the photomicrographs with a ring of dead cells visible around a small spheroid, not observed for the HCT116-R cells (Fig.4a).

(a)

(b)
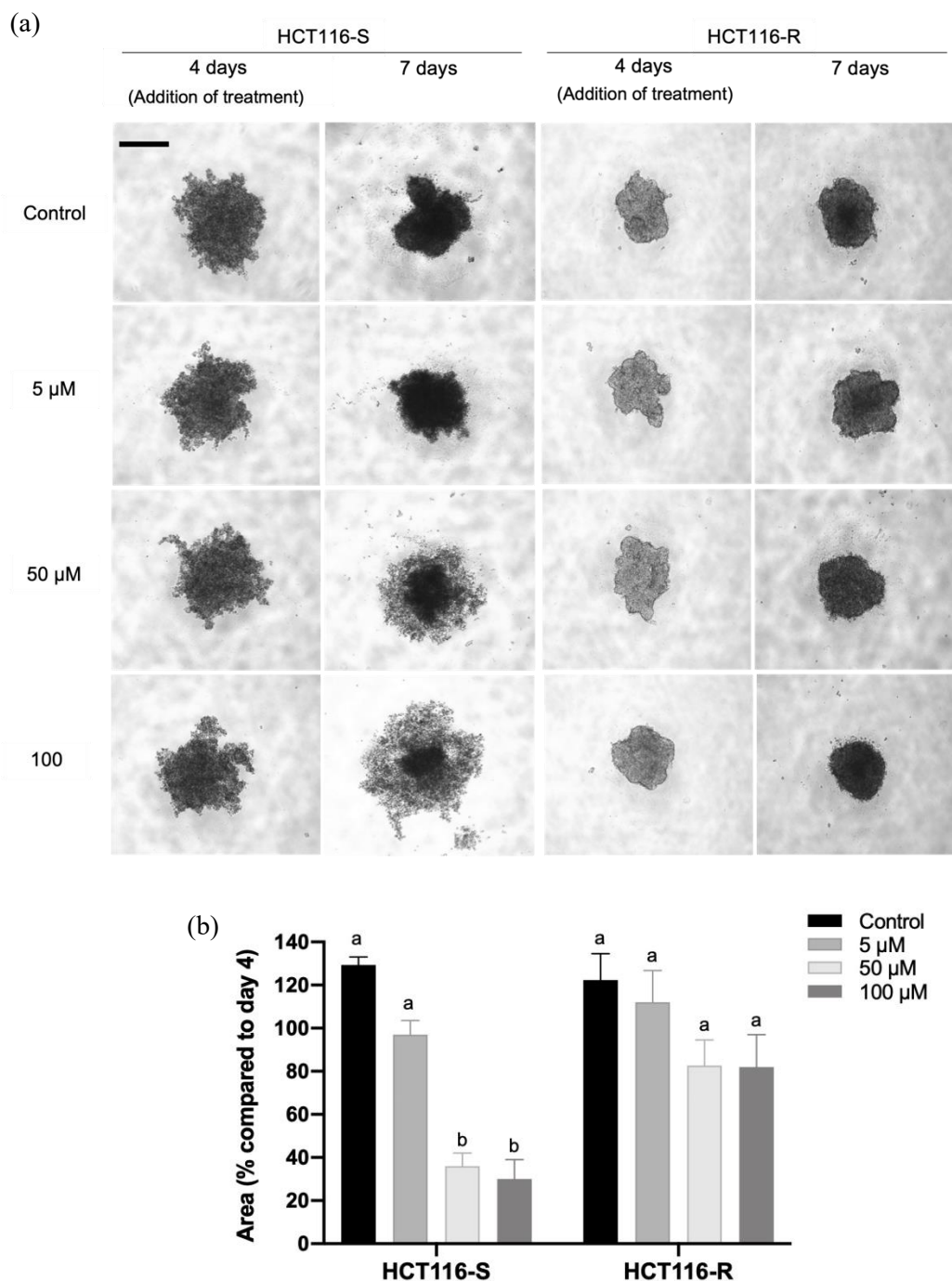
Figure4. Tumor spheroid formation assay. (a) Spheroid photomicrographs of HCT116-S and HCT116-R cells exposed to different concentrations of L-OHP. Scale bar: 200 μm. (b) Spheroid total area percentage in relation to the control after 3 days of exposure to the treatments, a total of 7 days of spheroid growth. Bars with different letters are statistically different (ANOVA two-way). Results expressed as mean ±SEM of3 independent experiments performed in triplicate.

Cell cycle analysis: flow cytometry

Flow cytometric analysis was performed to determine the cell-cycle profile. A total of 1×10^4 cells were recorded and the results are presented as mean percentage (±standard error, SD) of 2 independent experiments (Fig.5).

The proportion of cells in G0/G1 phase is increased for HCT116-R cells when compared with HCT116-S cells. As shown in Fig.5, the values for HCT116-S are 39.45% (±4.31), 18.90% (±0.57), 14.75%

(±1.48), and 17.70% (±0.57); and for HCT116-R: 43.10% (±1.56), 39.75% (±1.48), 49.60% (±0.85), 33.90% (±0.42), after a 48-h treatment with L-OHP 0, 5, 50, and 100 μM, respectively.

The HCT116-R cells did not present cells in the sub-G1 phase in the control group and group L-OHP 5 μM, 3.61% (±1.30) in group L-OHP 50 μM, 6.88% (±0.02) in group L-OHP 100 μM, after a 48-h treatment. Unlike the HCT116-R cells, the percentage of cells in the sub-G1 phase significantly increased for HCT116-S cells treated with L-OHP, as follows: 1.13% (±0.66), 31.50% (±3.82), 40.40% (±5.23), 33.50% (±2.26), after 48-h treatment with L-OHP 0, 5, 50, and 100 μM, respectively.

The proportion of HCT116-R cells in G2/M phase increased after exposure to 100μML-OHP when compared to the other concentrations, as follows: 23.65% (±14.35), 14.35% (±1.91), 23.15% (±0.78), and 44.35% (±18.60), after a 48-h treatment with 0, 5, 50, and 100 μM L-OHP, respectively.

Finally, it is possible to observe in Fig. 5a that the cell cycle pattern of HCT116-R treated with L-OHP at a concentration of 5 μM and 50 μM remains similar to the control group.
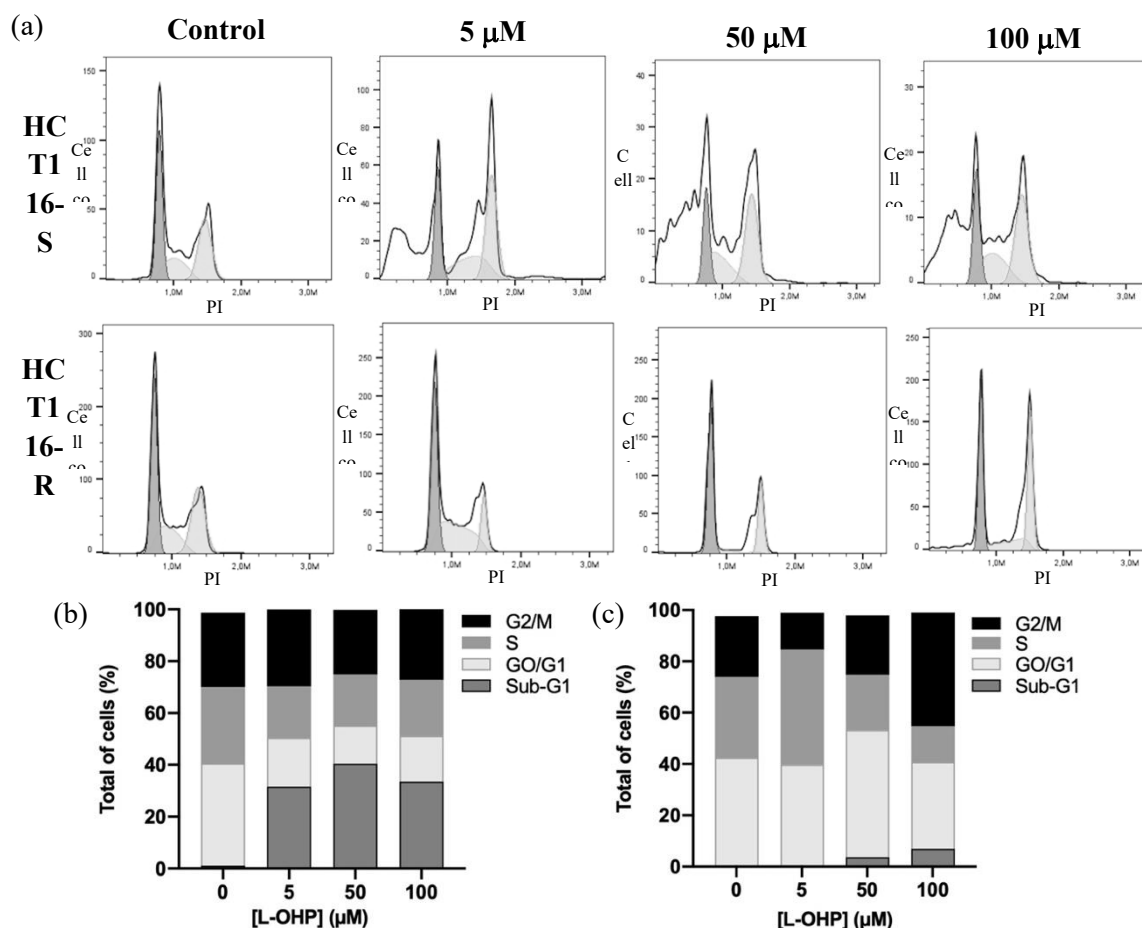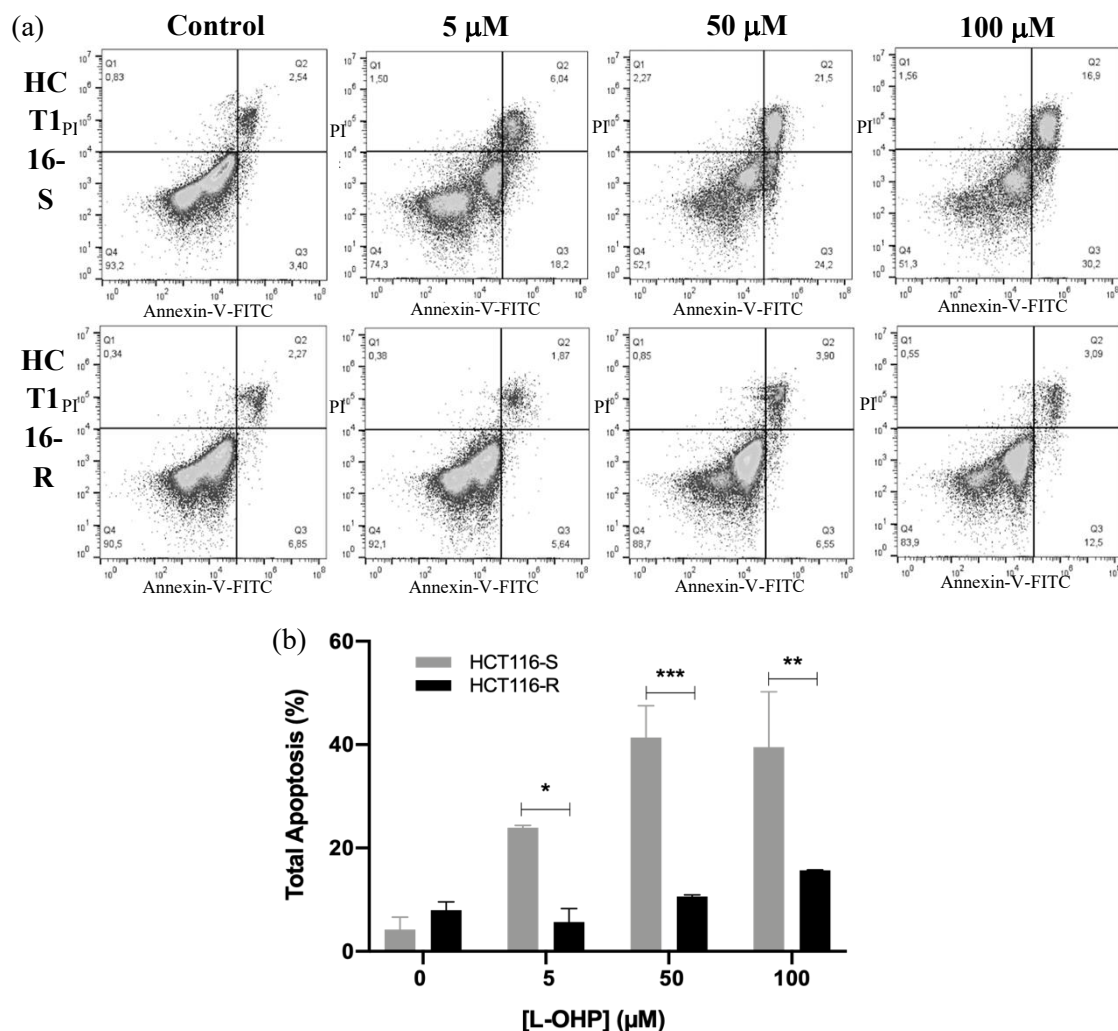

Figure5. Cell cycle analysis by flow cytometry. (a) Cell cycle profile of HCT116-S and HCT116-R cell lines exposed to different L-OHP concentrations for 48 h. The first peak represents the G0/G1 phase; the second peak represents the S phase, and the third peak represents the G2/M phase; (b) HCT116-S cell line treated with different L-OHP concentrations; (C) HCT116-R cell line treated with different L-OHP concentrations. Results expressed as the mean of 2 independent experiments.

Cell death analysis: flow cytometry

The cell death analysis of HCT116-S and HCT116-R exposed to different L-OHP concentrations for 48 h is represented in Fig.6. The results are expressed as the mean percentage (±SD) of 2 independent experiments. Exposure to L-OHP caused apoptosis in the HCT116-S cell line (Q2 and Q3), with 4.24% (±2.41), 23.92% (± 0.46), 41.35% (± 6.15), and 39.50% (±10.75)after a 48-h treatment with 0, 5, 50, and 100 μM L-OHP, respectively. HCT116-R showed higher cell viability (Q4) and a lower apoptosis rate (Q2 and Q3) independent of the L-OHP concentration used, such as 7.99% (±1.60), 5.67% (±2.61), 10.64% (±0.27), and 15.67% (±0.11)for 0, 5, 50, and 100 μM, respectively. These results corroborated the previous viability assays and

suggested a significant resistance of the HCT116-R cell line to L-OHP, which seems to develop mechanisms to evade apoptosis.

Figure6. Cell death analysis by flow cytometry. (a) Cell death profile of HCT116-S and HCT116-R cell lines exposed to different L-OHP concentrations for 48 h; (b) Total apoptosis analysis (Q2 and Q3). Results expressed as mean ±SE (standard error) of 2 independent experiments. ANOVA two-way: *P<0.05; **P<0.01; ***P<0.001

IV. DISCUSSION

The protocol employed, involving prolonged exposure and gradually increasing L-OHP, is feasible and allowed us to obtain a significantly chemoresistant cell line, confirmed by the increased OHP IC50 value which was 10 times greater for the resistant cell line than the sensitive/parental cell line. The time taken to obtain HCT116-R cells with a drug resistance index (DRI) equal to 10.2±1.0 was similar to that reported by ZHANG et al[31], approximately 9.4 months and DRI 10.78 for the L-OHP-resistant HCT-8 CRC cell line.

The cells herein were cultured for 40 passages until they reached the final resistance value stated which is also consistent with data in the study by JENSEN et al[34], in which the 3 CRC cell lines used (HCT116; HT29; LoVo) in the last exposure to L-OHP were between passages 41 and 47. Therefore, it is a similar passage number to the resistance induction protocols involving prolonged and gradual exposure to L-OHP.

Here we showed that the HCT116-R cell line (doubling time: 26.89±0.8 h) has a slower growth rate compared to the HCT116-S cell line (doubling time: 19.29±0.9 h). The changes in the growth rate after L-OHP resistance acquisition were also reported by KHOURY et al[26], in a study comparing the growth of parental and resistant cells using MTT and flow cytometry, in which the authors demonstrated that L-OHP resistant HT29 cells grew slower than the parental cells. In addition, the authors observed a similar change in growth rate in doxorubicin-resistant HCT116 cells compared to parental cells.

Similar to our findings, LIU et al[35] developed 2 L-OHP-resistant CRC cell lines (SW620/L-OHP and loVo/L-OHP cells) after a prolonged and gradually increasing exposure to L-OHP, totaling 10 months and more

than 100 passages to obtain the final cell lines. Corroborating our results, the authors also evidenced changes in the doubling time of resistant cells (SW620/L-OHP cells: 34.94 h; loVo/L-OHP cells: 28.11 h), which became slightly slower than the sensitive cells (SW620 cells: 29.53 h; loVo cells: 24.77 h).

The real-time growth of cells exposed to different L-OHP concentrations showed us that there is a difference in the growth curve of each cell line. The HCT116-S cells grow at a faster rate and die after a duration exposed to any concentration of L-OHP. In contrast, HCT116-R cells grow more slowly when exposed to lower L-OHP, concentrations but stop growing at higher concentrations and seem to enter a steady state. The steady state observed herein may be related to entry into the senescence state, as described by WAS et al[36]. These authors demonstrated that cells exposed to chemotherapy possess this characteristic as a drug defense mechanism which relates to the clinical observation involving tumor reoccurrence a short while after the completion of treatment.

Corroborating our findings, ALMENDRO et al[37] developed 3 L-OHP-resistant CRC cell lines and demonstrated that the modified cells were more resistant to apoptosis when exposed to chemotherapy. Our results suggest that HCT116-R cells also evade apoptosis, even when exposed to higher L-OHP concentrations. Conversely, HCT116-S cells exposed to higher L-OHP concentrations demonstrated a high apoptosis rate and an increased percentage of sub-G1 phase, in addition to a significant difference in spheroid integrity, with the presence of an evident ring of dead cells around the spheroid and a reduction in the final total area.

Cell cycle analysis indicated an increased percentage of HCT116-R cells in the G0/G1 phase, different from the HCT116-S cells. It is noteworthy that cells stop growing in the G0 phase and initiate the cell cycle in the G1 phase, so the increase in this proportion of cells corresponds to the arrest of cell growth[35,38-41]. The G2/M phase, a DNA damage checkpoint, ensures that cells repair damaged DNA or arrest proliferating, maintaining genomic stability, which is commonly increased in cells treated with platinum-based drugs, leading to apoptosis[35,38,42].

SU et al[41] demonstrated that their developed HCT116/L-OHP-resistant cells (DRI 9.4) were mainly composed of the G1 phase, which decreased after combined L-OHP and erianin treatment with and significantly increased the proportion of cells in G2/M phases, indicating a reversal of L-OHP resistance. In addition, YANO et al[43] demonstrated that invading cancer cells were usually in the GO/G1 phase, associated with a resistant profile against cytotoxic chemotherapy, and possessed a faster migratory capacity when in the G0/G1 phase than cancer cells in S/G2/M phases.

As observed herein, LIU et al[35] showed a higher proportion of cells in G0/G1 phase and a lower proportion in G2/M phase for their 2 L-OHP-resistant cell lines (SW620/L-OHP and loVo/L-OHP) when compared to the parental cell line, a finding the authors associated with the development of a stem cell-like phenotype and an MDR profile. It is known that chemotherapeutic resistant cells can develop several MDR mechanisms, such as drug inactivation, changes in drug target sites, increased DNA repair, increased expression of resistance-related genes, alterations in cell cycle, high expression of drug efflux pumps, and inhibition of cell death by apoptosis suppression[41,44,45].

The apoptosis evasion after L-OHP treatment of the HCT116-R observed in our work may suggest development relating to L-OHP resistance acquisition: an increase in DNA repair proteins removing the platinum-DNA adducts, modulation of cell cycle regulatory proteins, or even greater tolerance to DNA adduct accumulation[18,38,40,45]. ZHANG et al[31] compared the resistant HCT-8 cell with its parental/sensitive cell. The authors demonstrated that the induction of resistance led to significant changes in the expression of genes and proteins related to the MDR profile, with increases in DNA repair protein (ERCC1), efflux pump (ABCB1 and ABCC1), and GSTP1, related to drug detoxification.

The characteristics relating to MDR profile acquisition open a range of possibilities for the use of this type of cell model. It allows the carrying out of studies aiming to use resistant cell lines to understand how these cells respond to treatment, which is essential in terms of contributing to the effectiveness of the therapeutic regimen.

Furthermore, this kind of model can be used to analyze the acquisition of cross-resistance to other drugs as demonstrated by LIU et al[35]. The authors found that the established cell lines not only showed resistance to L-OHP, but also to other chemotherapeutic drugs, such as 5- fluorouracil, etoposide, cisplatin, vincristine, and epirubicin. This possibility may contribute to a better understanding of the molecular mechanisms related to resistance and the study of new treatments that may contribute to reverting resistance to chemotherapeutics.

V. CONCLUSION

The model developed is viable to be reproduced and can be used to contribute to studies with different goals, including: MDR mechanisms; therapeutic responses to new treatments; new approaches in an L-OHP resistant model; understanding how a resistant tumor might be responding, and the molecular mechanisms behind that response.

VI. ACKNOWLEDGMENTS

REFERENCES

[1]. Binefa G, Rodríguez-Moranta F, Teule A, Medina-Haynas M. Colorectal cancer: from prevention to personalized medicine. World J Gastroenterol. 2014; 20(22):6786-808.
[2]. Brenner H, Kloor M, Pox CP. Colorectal cancer. Lancet. 2014; 383:1490–502.
[3]. Arvelo F, Sojo F, Cotte C. Biology of colorectal cancer. Ecancer. 2015; 9:520.
[4]. Bray F, Ferlay J, Soerjomataram I, Siegel RL, Torre LA, Jemal A. Global cancer statistics 2018: GLOBOCAN estimates of incidence and mortality worldwide for 36 cancers in 185 countries. CA Cancer J Clin. 2018; 68(6):394-424.
[5]. Conde J, Oliva N, Zhang Y, Artzi N. Local triple-combination therapy results in tumour regression and prevents recurrence in a colon cancer model. Nat Mater. 2016; 15(10):1128-38.
[6]. Hu T, Li Z, Gao CY, Cho CH. Mechanisms of drug resistance in colon cancer and its therapeutic strategies. World J Gastroenterol. 2016; 22(30):6876-89.
[7]. Yu IS, Cheung WY. Metastatic Colorectal Cancer in the Era of Personalized Medicine: A More Tailored Approach to Systemic Therapy. Can J Gastroenterol Hepatol. 2018; 2018:9450754.
[8]. Zheng Y, Zhou J, Tong Y. Gene signatures of drug resistance predict patient survival in colorectal cancer. Pharmacogenomics J. 2015; 15(2): 135–143.
[9]. Modest DP, Pant S, Sartore-Bianchi A. Treatment sequencing in metastatic colorectal cancer. Eur J Cancer. 2019; 109:70-83.
[10]. Quere P, Facy O, Manfredi S, Jooste V, Faivre J, Lepage C, et al. Epidemiology, Management, and Survival of Peritoneal Carcinomatosis from Colorectal Cancer: A Population-Based Study. Dis Colon Rectum. 2015; 58(8):743-52.
[11]. Torres OJ, Marques MC, Santos FN, Farias IC, Coutinho AK, Oliveira CVC, et al. Brazilian consensus for multimodal treatment of colorectal liver metastases. Module 3: controversies and unresectable metastases. Arq Bras Cir Dig. 2016; 29(3):173-179.
[12]. Liu H, Xu Y, Zhang Q, Li K, Wang D, Li S, et al. Correlations between TBL1XR1 and recurrence of colorectal cancer. Sci Rep. 2017; 7:44275.
[13]. Seebauer CT, Brunner S, Glockzin G, Piso P, Ruemmele P, Schlitt HJ et al. Peritoneal carcinomatosis of colorectal cancer is characterized by structural and functional reorganization of the tumor microenvironment inducing senescence and proliferation arrest in cancer cells. Oncoimmunology. 2016; 5(12):e1242543.
[14]. Gelli M, Huguenin JF, Cerebelli C, Benhaim L, Honoré C, Elias D, et al. Strategies to prevent peritoneal carcinomatosis arising from colorectal cancer. Future Oncol. 2017; 13(10):907-918.
[15]. Benson AB 3rd, Venook AP, Cederquist L, Chan E, Chen YJ, Cooper HS, et al. Colon Cancer, Version 1.2017, NCCN Clinical Practice Guidelines in Oncology. J Natl ComprCancNetw. 2017; 15(3):370-398.
[16]. Van der Jeught K, Xu HC, Li YJ, Lu XB, Ji G. Drug resistance and new therapies in colorectal cancer. World J Gastroenterol. 2018; 24(34): 3834–3848.
[17]. Raymond E, Faivre S, Chaney S, Woynarowski J, Cvitkovic E. Cellular and molecular pharmacology of oxaliplatin. Mol Cancer Ther. 2002; 1: 227–35.
[18]. Howells LM, Sale S, Sriramareddy SN, Irving GR, Jones DJ, Ottley CJ, et al. Curcumin ameliorates oxaliplatin-induced chemoresistance in HCT116 colorectal cancer cells in vitro and in vivo. Int J Cancer. 2011; 129(2):476-86.
[19]. Alian OM, Azmi AS, Mohammad RM. Network insights on oxaliplatin anti-cancer mechanisms. Clin Transl Med. 2012; 1(1):26.
[20]. Perego P, Robert J. Oxaliplatin in the era of personalized medicine: from mechanistic studies to clinical efficacy. Cancer ChemotherPharmacol. 2016; 77(1):5-18.
[21]. Virag P, Fischer-Fodor E, Perde-Schrepler M, Brie I, Tatomir C, Balacescu L, et al. Oxaliplatin induces different cellular and molecular chemoresistance patterns in colorectal cancer cell lines of identical origins. BMC Genomics. 2013; 14:480.
[22]. Martin LP, Hamilton TC, Schilder RJ. Platinum Resistance:The Role of DNA Repair Pathways. Clin Cancer Res. 2008; 14(5):1291-5.
[23]. Ceballos MP, Rigalli JP, Cere LI, Semeniuk M, Catania VA, Ruiz ML. ABC Transporters: Regulation and Association with Multidrug Resistance in Hepatocellular Carcinoma and Colorectal Carcinoma. Curr Med Chem. 2019; 26(7):1224-1250.
[24]. Gottesman MM, Fojo T, Bates SE. Multidrug resistance in cancer: role of atp-dependent transportes. Nat Rev Cancer. 2002; 2(1):48-58.
[25]. Gillet JP, Gottesman MM. Advances in the molecular detection of ABC transporters involved in multidrug resistance in cancer. Curr Pharm Biotechnol. 2011; 12:686– 692.
[26]. Khoury FE, Corco L, Durand S, Simon B, Jossic-Corcos CL. Acquisition of anti-cancer drug resistance is partially associated with cancer stemness in human colon cancer cells. Int J Oncol. 2016; 49(6):2558-2568.
[27]. Porras VC, Bystrup S, Martínez-Cardús A, Pluvinet R, Sumoy L, Howells L, et al. Curcumin mediates oxaliplatin-acquired resistance reversion in colorectal cancer cell lines through modulation of CXC-Chemokine/NF-κB signalling pathway. Sci Rep. 2016; 6:24675.
[28]. Amaral MVS; Portilho AJS; Silva EL; Lívia OS; Maués JHS; Moraes MEA, et al. Establishment of Drug-resistant Cell Lines as a Model in Experimental Oncology: A Review. Anticancer Res. 2019; 39(12):6443-6455.
[29]. Han W, Yin H, Ma H, Wang Y, Kong D, Fan Z. Curcumin Regulates ERCC1 Expression and Enhances Oxaliplatin Sensitivity in Resistant Colorectal Cancer Cells through Its Effects on miR-409-3p. Evid Based Complement Alternat Med. 2020; 2020:8394574.
[30]. Mosmann T. Rapid colorimetric assay for cellular growth and survival: application to proliferation and cytotoxicity assays. J Immunol Methods. 1983; 65(1-2):55-63.
[31]. Zhang Y, Xu Z, Sun Y, Chi P, Lu X. Knockdown of KlK11 reverses oxaliplatin resistance by inhibiting proliferation and activating apoptosis via suppressing the Pi3K/aKT signal pathway in colorectal cancer cell. Onco Targets Ther. 2018; 2018:11 809–82.
[32]. Roth V. 2006. Doubling Time Computing. Available in: http://www.doubling-time.com.
[33]. Friedrich J, Seidel C, Ebner R, Kunz-Schughart LA. Spheroid-based drug screen: considerations and practical approach. Nat Protoc. 2009; 4(3):309-24.
[34]. Jensen NF, Stenvang J, Beck MK, Hanáková B, Belling KC, Do KN; et al. Establishment and characterization of models of chemotherapy resistance in colorectal cancer: Towards a predictive signature of chemoresistance. Mol Oncol. 2015; 9(6):1169-85.
[35]. Liu Z, Qiu M, Tang QL, Liu M, Lang N, Bi F. Establishment and biological characteristics of oxaliplatin-resistant human colon cancer cell lines. Chin J Cancer. 29(7):661-7. 2010.

[36]. Was H, Czarnecka J, Kominek A, Barszcz K, Bernas T, Piwocka K, et al. Some chemotherapeutics-treated colon cancer cells display a specific phenotype being a combination of stem-like and senescent cell features. Cancer BiolTher. 2018; 19(1):63-75.

[37]. Almendro V, Ametller E, García-Recio S, Collazo O, Casas I, Augé JM, et al. The role of MMP7 and its cross-talk with the FAS/FASL system during the acquisition of chemoresistance to oxaliplatin. PLoS One. 2009; 4(3):e4728.

[38]. Atallah D, Marsaud V, Radanyi C, Kornprobst M, Rouzier R, Elias D, et al. Thermal enhancement of oxaliplatin-induced inhibition of cell proliferation and cell cycle progression in human carcinoma cell lines. Int J Hyperthermia. 2004; 20(4):405-19.

[39]. Montopoli M, Ragazzi E, Froldi G, Caparrotta L. Cell-cycle inhibition and apoptosis induced by curcumin and cisplatin or oxaliplatin in human ovarian carcinoma cells. Cell Prolif. 2009; 42(2):195-206.

[40]. Feng R, Dong L. Knockdown of microRNA-127 reverses adriamycin resistance via cell cycle arrest and apoptosis sensitization in adriamycin-resistant human glioma cells. Int J Clin Exp Pathol.2015; 8(6):6107-16.

[41]. Su S, Liu SQ, Ma XY, Liu JJ, Liu JW, Lei M, et al. The effect and mechanism of erianin on the reversal of oxaliplatin resistance in human colon cancer cells. Cell Biol Int. 2021; 45(12):2420-2428.

[42]. Stark GR, Taylor WR. Analyzing the G2/M checkpoint. Methods Mol Biol. 2004; 280:51-82.

[43]. Yano S, Miwa S, Mii S, Hiroshima Y, Uehara F, Yamamoto M, et al. Invading cancer cells are predominantly in G0/G1 resulting in chemoresistance demonstrated by real-time FUCCI imaging. Cell Cycle. 2014; 13(6):953-60.

[44]. Szakács G, Paterson JK, Ludwig JA, Booth-Genthe C, Gottesman MM. Targeting multidrug resistance in cancer. Nat Rev Drug Discov. 2006; 5(3):219-34.

[45]. Mansoori B, Mohammadi A, Davudian S, Shirjang S, Baradaran B. The Different Mechanisms of Cancer Drug Resistance: A Brief Review. Adv Pharm Bull. 2017; 7(3):339-348.